

# Highly Controllable Ambient Atmosphere Spray Deposition of Water Dispersible Poly(Benzimidazobenzophenanthroline) Films

Mikko Salomäki<sup>a,c,\*</sup>, Oskari Jaakkola<sup>a</sup>, Sami-Pekka Hirvonen<sup>b</sup>, Heikki Tenhu<sup>b</sup>, Carita  
Kvarnström<sup>a,c</sup>

<sup>a</sup>Department of Chemistry, University of Turku, Finland

<sup>b</sup>Polymers and Colloids group, Materials Chemistry, Department of Chemistry, University of  
Helsinki, Finland

<sup>c</sup>Turku University Centre for Materials and Surfaces, Turku, Finland

\*Corresponding author, email:mikko.salomaki@utu.fi

## Abstract

Thin films of water dispersible poly(ethylene oxide) (PEO) functionalized poly(benzimidazobenzophenanthroline) (BBL) polymers have been prepared by a pulse spray technique on a spinning substrate in ambient atmosphere. The deposition method is advantageous for generating ultra-thin films of nanometer thicknesses. A single spray pulse was found in a reproducible manner to generate a layer of ca. 2 nm thickness. The PEO-chain length in the BBL functionalization had an essential influence on the building mechanism of

the films. The polymers functionalized by short PEO chains induced the formation of very smooth films while longer PEO chains induced rough films and notable nanostructuring. The BBL-PEO film deposited using spray pulse deposition was found to be electro- and photoactive. The electron transfer processes observed are slightly different from earlier reported results for similar polymers, which is probably due to the very thin film. The films exhibited photocurrent generation when transformed into conducting form.

Keywords: poly(benzimidazobenzophenanthroline); Spray deposition; electroactive films; photoactive films

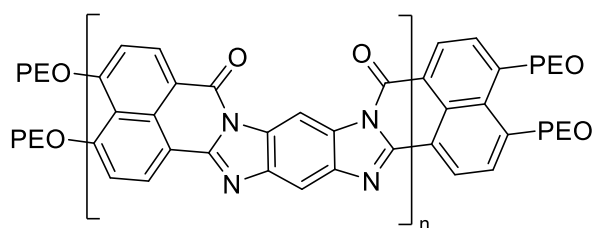
## Introduction

Poly(benzimidazobenzophenanthroline) (BBL) is an aromatic ladder-type conjugated polymer which has been synthesized already in late 1960's[1,2] and has since then been actively studied.[3-7] The BBL's molecular structure is planar due to its rigid backbone and possesses high chemical and thermal stability[8] as well as high electron affinity.[9] BBL can be utilized as an n-type conducting film in for example optoelectronic devices, where there is a demand for stable n-type organic semiconductors.[10] The use of BBL in photovoltaics and organic transistors is already reported in literature.[11-22] Previously BBL was proven an effective photoanode material for water oxidation.[23]

Organic materials have been used progressively in electronics (solar cells, OFETs, OLEDs, etc.). The deposition processes of thin organic films when utilized in devices highly affects the function of the device. In order to improve device performance, there is a need of new approaches to deposit films of high homogeneity and precise thickness control. Advanced thin

film devices are essentially multilayer structures where all layers should be processed without affecting the underlying layers, which remains a challenge in multilayer assemblies. On the other hand, devices consist of multilayer structures where each layer in the stack can be conveniently deposited by an individual technique. Spin-coating persists the most widely used liquid phase deposition technique. Nevertheless, the method cannot be used for large area devices and there are problems when the multilayered materials are soluble in the same solvents. Furthermore, the lack of control at nanoscale is usually considered as a major drawback in liquid phase deposition. One approach to conquering the problems is chemical vapor deposition and atomic layer deposition.[24] These rather expensive methods consume a lot of energy per deposited material, have slow growth rates and utilize custom-made precursor molecules. On the other hand, they usually ensure error free epitaxial growth in the atomic level with strong bonds between the molecules. Conducting polymer films are traditionally assembled via electrochemical deposition. However, the method is not applicable to BBL due to lack of appropriate monomer. Another significant drawback in the utilization of BBL is insolubility, as such, in practically any common solvent. Methanesulfonic acid is an exception, which has been found to dissolve BBL.[9] The methanesulfonic acid solution can be transformed into an aqueous nanofiber dispersion, which can be utilized in preparation of thin BBL-films.[23,25,26] In addition, stable dispersions and high colloidal stability in aqueous solutions can also be achieved by substituting poly (ethylene oxide) (PEO, Scheme 1)[27] and poly(N-isopropylacrylamide)[28] in the chain ends of BBL. The PEO substitution does not significantly alter the electrical and optical properties of BBL.[6] Furthermore, the substitution facilitates the processability in water dispersion, which can be utilized in straightforward thin film deposition. BBL-PEO has been shown to be suitable for composite material formed with a p-type polymer.[29]

We have previously constructed a deposition system where spraying is applied onto a substrate during high-speed spinning.[30] Spraying allows very fast wetting of the surface of a substrate with a minimal amount of solution, even less than what is used in a single step of spin coating. In a spinning motion, the draining and drying of the substrate is promoted by centrifugal force. Therefore, very rapid successive spray steps are then possible. Centrifugal force also minimizes the effect of surface tension so the drop boundaries, which are sometimes considered problematic in spraying applications, are not observed in high speed spinning substrate.[30] In this paper we utilize a deposition of water dispersible BBL derivatives using short aerosol pulses sprayed towards a spinning substrate. The aim of this approach is to obtain smooth, defect-free and uniform thin BBL films using inexpensive, vacuum-free process that is applicable to multilayer assemblies.



Scheme 1. Common structure of poly(benzimidazobenzophenanthroline)- poly(ethylene oxide) (BBL-PEO) polymers used in this paper.

## Experimental Section

### The substrates and materials

The substrates (quartz plates (Alfa Aesar), silicon wafers and fluorine doped tin oxide glass (SnO<sub>2</sub>, K Glass from Pilkington)) were cleaned using H<sub>2</sub>O<sub>2</sub>:NH<sub>3</sub>:H<sub>2</sub>O (1:1:5) solution, rinsed with water, dried, and silanized using a 5% (v/v) solution of N-(trimethoxysilylpropyl)-N,N,N-triethylammonium chloride (ABCR) in methanol for 5 minutes. The BBL-PEOs used were

synthesized earlier and the detailed synthesis and characterization is described elsewhere [27]. BBL derivatives were used as 1.5 mg/ml water dispersions. Before deposition, the dispersions were homogenized for 15 minutes using a tip sonicator (Hielscher UP100H). After that, the dispersions were centrifuged for 15 minutes in 3000 g for separating remaining aggregated particles.

### The spraying system

The spraying system (Figure 1) constituted of on house made air-atomizing nozzle made of polytetrafluoroethylene (PTFE). The air channel inside the nozzle was 2 mm and polyether ether ketone (PEEK) tube (1.6 mm outer diameter) for liquid feed was fitted inside the air channel. The nozzle was driven with 200 kPa pressurized air. The liquid was pushed from the container using 30 kPa overpressure in order to achieve a steady liquid flow. A uniform spray cone was generated by opening the solenoid valve (NRResearch) after the liquid container while the air was constantly driven through the channel. A single spray pulse for the duration of 100 ms consumed ca. 35  $\mu$ l of solution. Drying of the spinning substrate took place within one second, but for repeatability, a five-second delay was kept in between the successive pulses. Spraying time was controlled using LABVIEW software (National Instruments) and the interface board (National Instruments USB-6008). Spraying was applied on a substrate attached to the spinner (Pine instrument company) having adjusted spinning speed of 5000 rpm. After the deposition, the BBL films were annealed at 70°C for one hour.

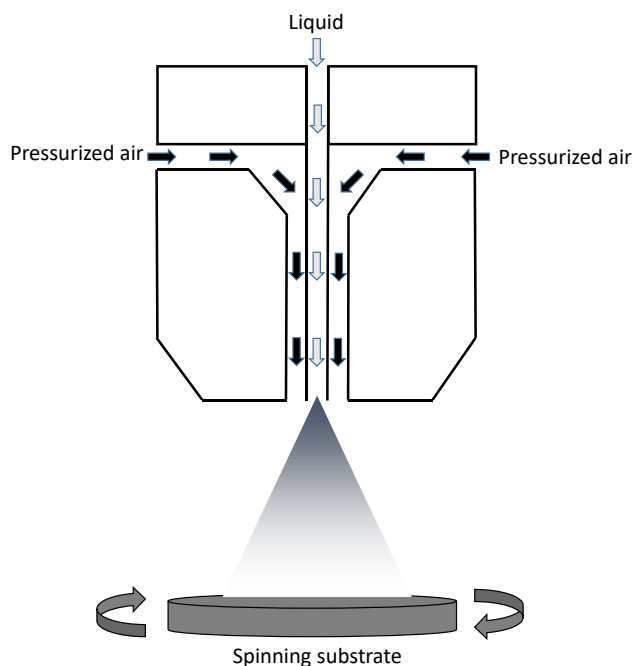


Figure 1. Scheme of the spraying nozzle.

### Characterization of films

The UV-Vis spectra were measured by HP 8453 spectrometer. Atomic force microscopy, AFM (diCaliber AFM, Bruker), operated in the tapping mode was used to measure the topography and the root mean square roughness of each film deposited on silicon. The films were also scratched with a doctor blade in order to get an estimate of the film thickness. The morphology of the films was also studied by scanning electron microscopy, SEM (LEO Gemini 1530)

The ellipsometric analysis of a polymer film on silicon was carried out using EP3 spectroscopic and imaging ellipsometer (Accurion). Xe lamp was used in the spectral range of 370–950 nm. The ellipsometric spectra were analyzed using EP4Model modeling software (Accurion) with the following optical model: Si/SiO<sub>2</sub>/BBL/BBL(rough). Tauc-Lorentz model[31] was used in modeling BBL and Bruggemann effective medium for modelling rough surface layer.

Electrochemical characterization was carried out in a conventional three-electrode one-compartment cell using cyclic voltammetry (CV) and an Iviumstat potentiostat. The cell was filled with 0.1 M tetrabutylammonium hexafluorophosphate in acetonitrile. The working electrode for CV experiments was FTO coated glass and a platinum wire was used as a counter electrode. An AgCl coated Ag wire was used as quasi-reference electrode and all potentials reported are vs. this electrode. The Ag/AgCl electrode was calibrated vs. ferrocene ( $\text{Fe}/\text{Fe}^+$ ) ( $E_{1/2}(\text{Fe}/\text{Fe}^+) = 0.45 \text{ V}$ ) before each experiment

Photocurrent generation in the thin films were studied using white LED and 590 nm LED illumination (Ivium ModuLight) having power densities of  $16 \text{ mW}/\text{cm}^2$  and  $1.6 \text{ mW}/\text{cm}^2$  respectively measured with a calibrated photodiode. The illumination was carried out from the backside of the glass plate using the same three-electrode cell filled with the same electrolyte solution as in CV measurements. The system was analyzed in forward bias and in an open circuit mode. To rule out possible interferences a blank FTO-glass plate with electrolyte solution was analyzed by light on-light off measurement.

## Results and discussion

### Deposition and optical characterization of films

Four different combinations of BBL-PEO polymers were selected for this study. The descriptions of abbreviations are given in Table 1. BBL1 and BBL2 represent polymers with short PEO chains (Mw 750) and BBL3 and BBL4 have long PEO chains (Mw ca.2000). The BBL length varied from 1700 to 6700 Mw. All four polymers were sprayed on silanized quartz

substrates using ten spray pulses on a spinning substrate. Figure 2 shows the UV-Vis absorbance generated by the deposited films. The absorbance near 355 and 585 nm are characteristic of the BBL polymer.[32] The effect of PEO-chains on the ratio of the two aforementioned BBL absorbance bands is clearly visible.[32] The ratio of intensities of absorbance values at 585 vs. 355 nm is roughly 1 in the polymers functionalized with short PEO chains and 0.8 in the polymers functionalized with long PEO chains. A decrease in the 585 nm band is accredited to orientational interference of BBL conjugation as a result of influence of PEO chains.[32] In spite of having large variation in the BBL:PEO ratios between the polymers, the effect of BBL:PEO ratio is not clearly seen in the absorbance bands. The polymers functionalized with short PEO chains seemed to produce films with higher BBL-absorbance comparing with the polymers functionalized with long PEO chains. Accordingly, the most influential factor in the film construction appears to be the length of the PEO chain.

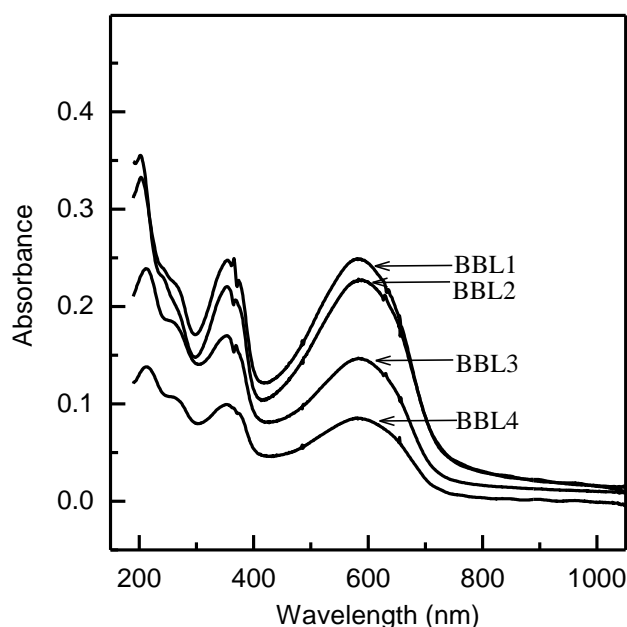


Figure 2. UV-Vis spectra of BBL-films deposited using 10 spray pulses on quartz plate.



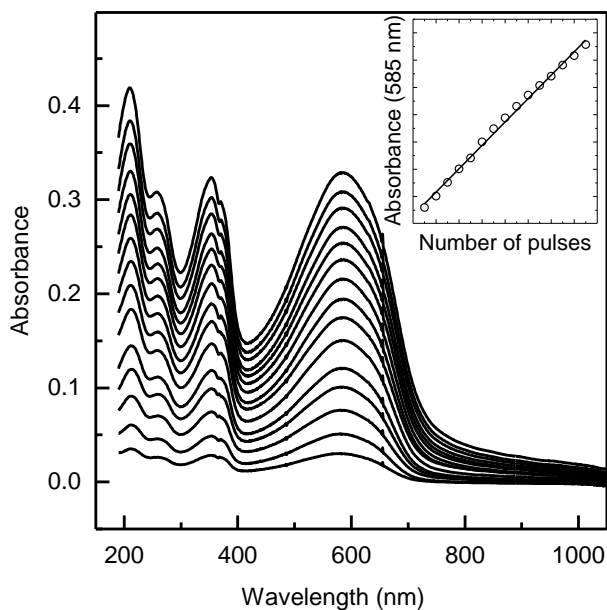


Figure 3. Spectra of evolution of absorbance of a BBL1 film after individual spray pulses. The quartz plate was detached from the spinner and measured after each spray step. The inset shows the absorbance at 585 nm vs. the number of deposition steps.

In a comprehensive measurement of absorbance of a BBL film, (Figure 3) a spectrum of the film was measured after each spray pulse of BBL1 polymer. The figure shows the development of absorbance during the sequential spray and measurement cycles. The most noticeable feature in the graph is that the absorbance appears to grow perfectly linearly with the number of spray pulses during the monitored period of 15 spray pulses. The figure inset emphasizes the linearity of the absorbance at 585 nm versus the number of pulses. The average increase in absorbance per layer is ca. 0.02.

In order to study the optical properties of the film, a BBL1 film was deposited using 10 spray pulses and examined by spectroscopic ellipsometry. BBL was assumed to follow Tauc-Lorentz model[31,33], which is generally used to model the dielectric function of amorphous materials. Tauc-Lorentz oscillator is a refinement of the Lorentz oscillator by allowing the estimation of

the energy of the band gap. The calculation of the complex dielectric function assumes that the material is a compilation of individual non-interacting oscillators. The ellipsometric analysis was carried out based on two Tauc-Lorentz oscillators. It would have been possible to add more oscillators as it may have been justified on the basis of the absorption spectrum, but the utilized ellipsometer did not support UV-range. Therefore, the fitting of UV-bands was not applicable. The experimental psi and delta values from the measurement and the fitted data according to the optical model are shown in figure 4. The selected optical model satisfactorily fits the experimental values. The obtained thickness was 18 nm for the BBL layer and 2 nm for the rough surface layer. The oscillator energies obtained were 1.9 and 2.4 eV. The obtained optical band gap was 1.63 eV, which is well in agreement with the band gap estimated from the absorbance spectrum 1.65 eV. Previously estimated band gap for similar polymers, but for thicker films, was 1.7 eV.[6] For unsubstituted BBL the band gap is estimated to be 1.8 eV.[34] Therefore it can be stated that the influence of PEO functionalization only has minor effect on the properties of BBL.

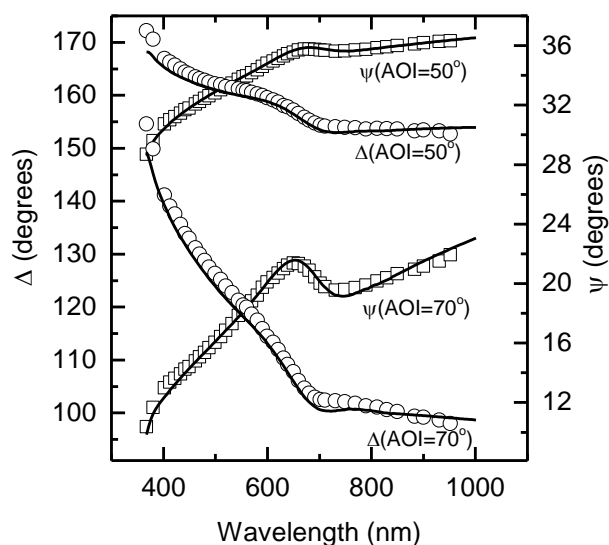


Figure 4. Ellipsometric spectra of a BBL1 polymer film on silicon. Spectra were recorded using two angles of incidence 50 and 70. Circles and squares represent the measured psi and delta angles, lines indicate the fitting results from the optical model.

#### Thickness and morphology of films

BBL-films that were deposited using 10 spray pulses on silicon substrates were analyzed by atomic force microscopy and scanning electron microscopy in order to distinguish the relationship between the polymer structure and film morphology. The results of thickness analysis using AFM are given in the Table 1. AFM and ellipsometric analysis of a BBL1 film combined with the absorbance data of stepwise deposition shown in figure 3 discloses that the film having the absorbance of 0.24 at 585 nm is ca. 19 nm thick. Consequently, it can be calculated that a single spray pulse in case of BBL1 increases the film thickness in a reproducible way by only two nanometers. This is an indication of a highly controlled deposition method. Furthermore, it would appear that film thicknesses obtained by AFM correlate by some means with the film absorbance at 585 nm. However, neither the absorption at 585 nm nor at 355 nm represent an optimal estimation of film thickness because the effect of PEO in the total volume of the film is not included in those bands. Additionally, the thickness analysis based on the band at 585 nm leads to false interpretation. That is because of the orientation disruption in BBL caused by PEO side chains as discussed earlier. Nevertheless, the best correlation between film thickness and absorbance is apparently obtained from the peak at 205 nm. The exact interpretation of the aforementioned peak is uncertain, but it is possible that it is a combinational band having the contribution of scattering and absorbance from both BBL and PEO domains.

Polymers functionalized with long PEO chains produce the thinnest films. However, at the same time they produce notably uneven surfaces. The root mean square (RMS) roughnesses of films of polymers functionalized with long PEO chains are notably higher than in films functionalized with short PEO chains. In addition, the roughness/thickness ratio, which can be considered as a factor of the film quality, is higher when the polymers having short PEO chains are deposited. In figure 5, representative thickness profiles of four different BBL films are listed. The effect of the PEO-chain length on film quality is clearly seen in the increasing roughness of the profiles.

Table 1. Designations of BBL derivatives and film parameters.

<b>Polymer</b>	<b>n(BBL)</b>	<b>M<sub>w</sub>(BBL)</b>	<b>M<sub>w</sub>(PEO)</b>	<b>BBL:PEO ratio</b>	<b>RMS roughness (nm)<sup>a</sup></b>	<b>Thickness (nm)<sup>a</sup></b>	<b>Roughness/thickness</b>
BBL1	20	6700	750	8.9	4.0	19	0.21
BBL2	5	1700	750	2.3	3.9	20	0.20
BBL3	20	6700	2000	3.4	6.7	15	0.45
BBL4	10	3300	1900	1.7	9.6	10	0.96

<sup>a</sup>Thickness and roughness of polymers films deposited using 10 spray pulses. RMS roughness is calculated from 50\*50 μm AFM image

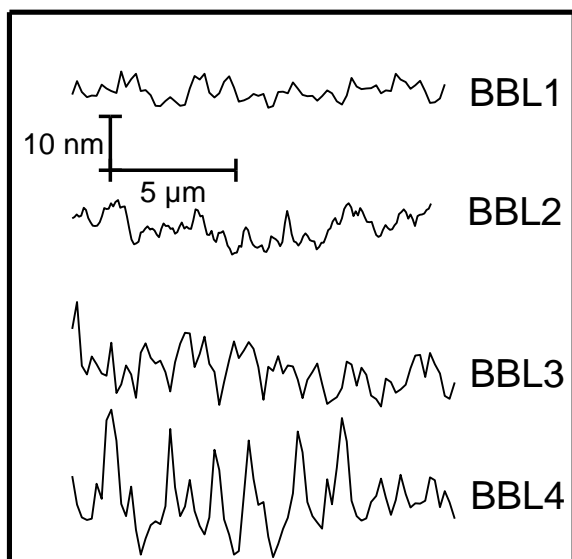


Figure 5. Surface profiles of BBL-films after ten spray cycles. Film roughness is measured by Atomic force microscopy. Thickness of the films are listed in the Table 1.

The scanning electron microscopy images of films reveal characteristic nanolevel structures on the surfaces of the films. The films where BBL has been functionalized with long PEO chains seem to have certain characteristic morphology in comparison to films where BBL has been functionalized with short PEO chains. Previously observed higher surface roughness in the film made of polymers having long PEO chains is recognized as nanobelt type aggregates that are especially visible in SEM images (figure 6). The polymer functionalized with long PEO and having a high percentage of PEO (BBL4) seems to form aggregates that are approximately a couple of tens of nanometers in width and up to micrometer in length. The same phenomenon has been observed in earlier studies.[32] The other polymer functionalized with long PEO chains but of a lower percentage (BBL3) seems to produce flake-like surface features. The film appears to be uniform but at the same time, it has higher roughness comparing with polymers functionalized with short PEO chains. BBL2 film seems almost completely featureless in the

SEM image (figure 6b), but in the BBL1 film (figure 6a) there is some structuration detectable. Despite that, the roughness of the latter mentioned films is quite low.

The stacking and aggregation of BBL:PEO polymers is presumed to be a combination of ability of BBL to form nanowire and nanobelt type aggregates and ability of PEO to form stable dispersion in solution. It seems that the polymers functionalized with short PEO chains favor fast reorganization on upon the contact between aerosol droplets and the surface bound material. Accordingly, the polymers functionalized with long PEO chains tend to maintain their intrinsic nanostructure on the film formation.

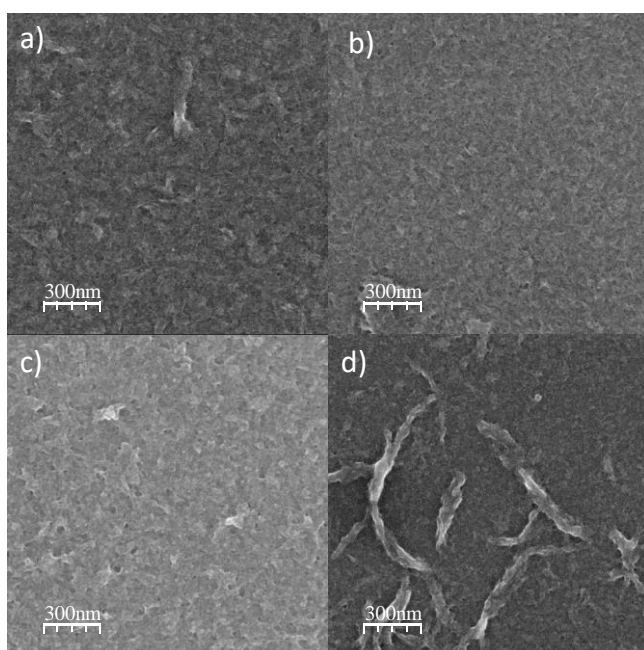


Figure 6. Scanning electron microscopy images of BBL1 (a), BBL2 (b), BBL3 (c), and BBL4 (d) films. The films are deposited using 10 spray pulses.

Electrochemical analysis and photocurrent generation

BBL1 was selected for electrochemical analysis because it develops the best quality films. The difference in the electrochemical behavior between the different combinations of BBL and PEO is not remarkable.[6] Approximately 15 nm thick BBL1 films, estimated from the absorbance at 585 nm, were studied by cyclic voltammetry (Figure 7). The mechanism of the reduction process of BBL is debated in the literature [9,35,36] and the previous analysis of similar BBL films showed two clearly separated reduction processes.[6] In earlier studies, the analysis of BBL-PEO was conducted on drop casted BBL films having their thickness in the micrometer range. Interestingly, ultrathin films undergo a reduction process, giving rise to only one sharp peak in the voltammogram and the transfer process of two electrons seem to take place at the same potential. The main reduction process of ultrathin film takes place approximately at the same potential as the latter reduction step in a thicker film.[6] In addition to that, annealing of the thick film has been found to change the current ratio of two observed reduction peaks so that the latter reduction current is increased.[6] Therefore, shift towards a single peak in a voltammogram is probably due to increasing compactness of the BBL-film. Comparable transformation towards a single peak has been observed previously when the pH of the solution was adjusted to below one[9], which was also found to increase the electrochemical stability of the film. In the ultrathin film, the voltammogram maintains its shape from the first cycle excluding a minor peak at -0.6 V. The change of reduction and oxidation potentials during ten successive scans is very small denoting a relatively high stability of the film. The corresponding LUMO level or electron affinity level was determined from the reduction potential onset value using the empirical relationship proposed by Brédas et al. using a scale factor of 4.4 eV relating Ag/AgCl to vacuum[37] giving a value of -3.4 eV. For non-functionalized BBL the LUMO level is estimated to be ca. -4.0 eV.[38] Furthermore, there is no need for pre-cycling to achieve representative voltammograms as it was in the case of thick films. The characteristic behavior of ultrathin BBL film is also partly accredited to

interfacial effect. The film is so thin that most of the material in the film is electroactive and located on the electrochemical interface enabling the steady diffusion of counter ions from the solution to the film. It is therefore directly accessible for electrochemical interface reactions. That also means that the amount of the inactive bulk material in the film is very low.

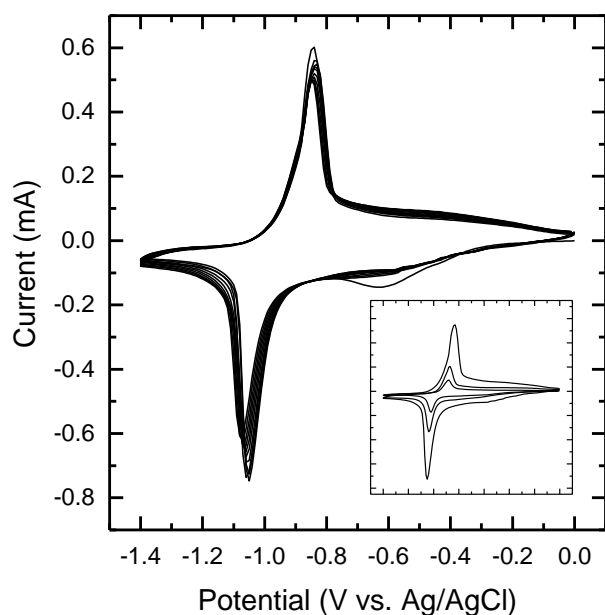


Figure 7. Cyclic voltammograms of BBL1-film on FTO-glass. Ten successive scans. Scan rate 50 mV/s. The inset shows cyclic voltammograms of films on FTO glass using different scanning speeds 10, 20 and 50 mV/s.

The band gap of BBL1 (1.63 eV) is appropriate for application of photoelectrochemical reactions. To determine the photogenerated processes sufficiently thick (40 nm) BBL1-film was deposited on transparent substrate. The film was electrochemically reduced and reoxidized several times in order to increase the doping level and the conductivity of the BBL-polymer. Forward bias was applied to the film. The BBL film shows anodic photocurrent upon white LED (16 mW/cm<sup>2</sup>) illumination (Figure 8). The shape of the photocurrent is slowly declining



during the illumination without charging and discharging spikes. The photocurrent arises most probably from water that is present in the moist acetonitrile and the electrolyte used in the electrochemical cell. Direct comparison of current densities to other studies of water oxidation [23] is in this case difficult because of different light source and solvent, but the capability of BBL as a photoanode material is clearly shown.

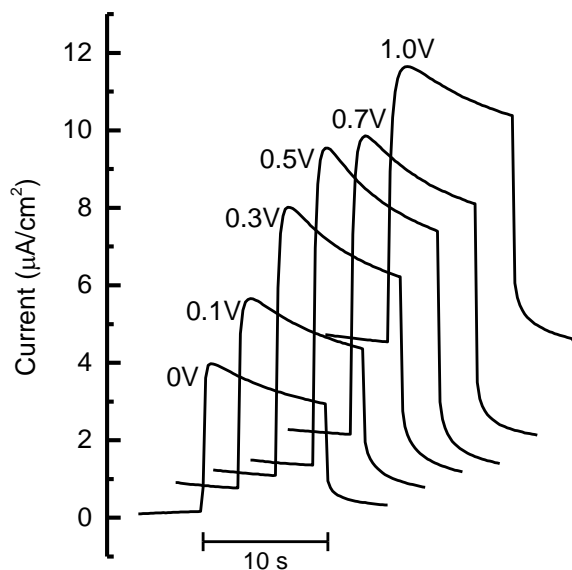
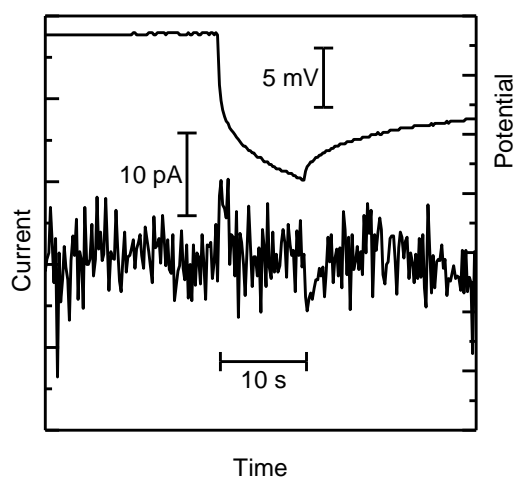


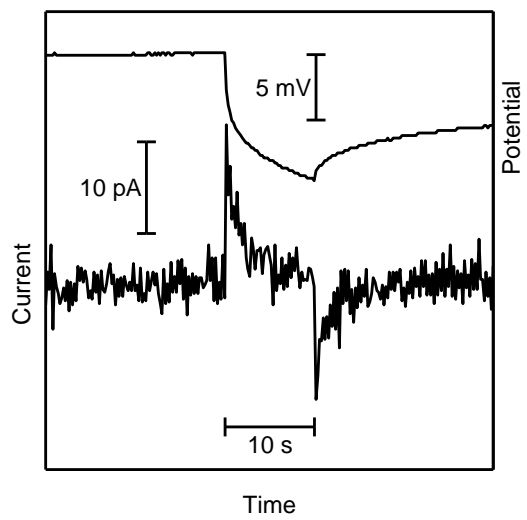
Figure 8. Current density of BBL1 under forward bias and chopped illumination. At each potential the film was allowed to stabilize for 20 seconds before the light was switched on for 10 seconds.

Upon irradiating pristine BBL1 film in an open circuit mode by 590 nm light pulses, no clearly detectable photocurrent was observed. There are some changes in the vicinity of the engagement of a light irradiation (Figure 9a.), but the signal/noise ratio is too low for the characterization of the behavior. In addition, a slight change in the floating potential was observed. However, after the successive electrochemical reduction and reoxidation of the film, a minor but noticeable open circuit photocurrent generation was observed (Figure 9b). Due to

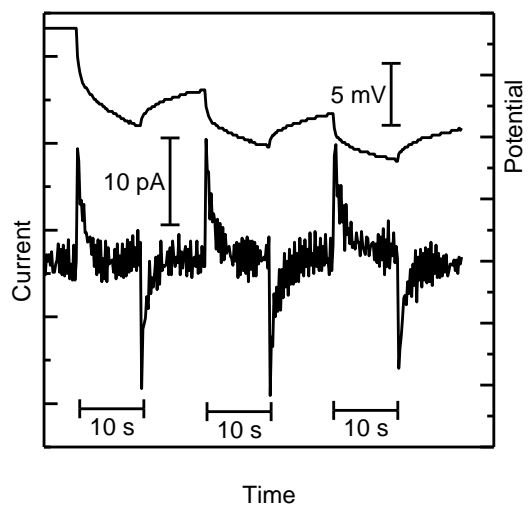
increased conductivity, the shape of the current development indicates that the film generates transient photocurrent. The steady state photocurrent is present but it is barely noticeable in the graph due to the low signal noise ratio. The potential change is comparable to the pristine polymer. The transient nature of the photocurrent is even more clearly seen in figure 9c where the film is irritated by three successive light pulses. When the light pulse is switched on, the photocurrent exhibits a sharp anodic peak. After that, there is an exponential drop to a steady state photocurrent. Directly after the light is switched off, a cathodic peak is detected, after which the current is leveled to the initial level. The sharp peaks are due to charging (anodic) and discharging (cathodic) of conducting BBL. The shape of the generated photocurrent can probably be explained by initial photocurrent generation in BBL and the lack of an electron mediator in the system. The intensity of photocurrent is influenced by relatively low intensity 590 nm LED with the power of  $1.6 \text{ mW/cm}^2$ . In addition to that, the transmittance of the thin film was approximately 30% at 590 nm. Nevertheless, this experiment reveals the photoactivity of bare BBL film in its conducting form.



a)



b)



c)

Figure 9. Photocurrent generation in BBL1 film. Designations: a) pristine film with single irradiation b) electrochemically reduced film with single irradiation, c) reduced film with multiple irradiations. 590 nm LED illumination and its duration is indicated in the figures.

## Conclusions

In summary, we have demonstrated that spray deposition is a practical and highly controllable method for the preparation of thin electro- and photoactive BBL-PEO films. The method is applicable to multilayer structures. Our study revealed that the BBL polymers modified with short PEO chains produced films with higher BBL-content comparing with the polymers modified with long PEO chains, but no clear correlation between the apparent amount of BBL and BBL:PEO ratio were observed. The most decisive factor in the film buildup was found to be the length of the PEO chain. The film thickness was found to increase perfectly linearly with the number of spray pulses. The average increase in film thickness with a steadily growing BBL:PEO polymer was estimated to be only two nanometers per spray pulse. Polymers functionalized with long PEO chains produced notably uneven surfaces with identifiable morphology. Apparently, the polymers functionalized with short PEO chains prefer fast reorganization on the substrate resulting in flat featureless conformation. On the contrary, the polymers functionalized with long PEO chains tend to maintain their intrinsic nanostructure on the film formation. The electrochemical reduction of ultrathin BBL-PEO film generated only a single current peak in the voltammogram. The previously recognized two-electron reduction appeared to take place at the same potential, resulting in one strong peak. This behavior is accredited to ultra-thin nature of the film. The film showed anodic photocurrent in forward bias. In an open circuit measurement, pristine BBL film did not show measureable photo

activity. However, after the successive electrochemical reduction and reoxidation of the film, a minor but noticeable transient photocurrent generation was observed.

In general, this deposition method is applicable to the assembly of ultra-thin films of functional molecules. The further studies on the deposition method are in progress. The necessary qualities for the deposited material are ability to quickly reorganize on the substrate and capability to intramolecular stacking interactions to aid uniform film formation. The method seems to favor suspensions and high viscosity solutions.

## References

- [1] FE Arnold, Vanduse.RI. Preparation and Properties of High Molecular Weight, Soluble Oxobenz[de]imidazobenzimidazoisoquinoline Ladder Polymer, *Macromolecules*. 2 (1969) 497-&.
- [2] FE Arnold, Vanduse.RI. Unusual Film-Forming Properties of Aromatic Heterocyclic Ladder Polymers, *J Appl Polym Sci*. 15 (1971) 2035-&.
- [3] XL Chen, SA Jenekhe. Bipolar conducting polymers: Blends of p-type polypyrrole and an n-type ladder polymer, *Macromolecules*. 30 (1997) 1728-1733.
- [4] T Yohannes, H Neugebauer, S Luzzati, M Catellani, SA Jenekhe, NS Sariciftci. Multiple electrochemical doping-induced insulator-to-conductor transitions observed in the conjugated ladder polymer polybenzimidazobenzophenanthroline (BBL), *J Phys Chem B*. 104 (2000) 9430-9437.
- [5] M Quinto, SA Jenekhe, AJ Bard. Polymer films on electrodes. 30. Electrochemistry and scanning electrochemical microscopy characterization of benzimidazolebenzophenanthroline-Type ladder (BBL) and semiladder (BBB) polymer films, *Chemistry of Materials*. 13 (2001) 2824-2832.
- [6] M Wagner, A Osterholm, S Hirvonen, H Tenhu, A Ivaska, C Kvarnstrom. Characterization of Water-Dispersible n-Type Poly(benzimidazobenzophenanthroline) Derivatives, *Macromolecular Chemistry and Physics*. 212 (2011) 1567-1574.

- [7] DJ Irvin, JD Stenger-Smith, GR Yandek, JR Carberry, DA Currie, N Theodoropoulou, et al. Enhanced electrochemical response of solution-deposited n-doping polymer via cocasting with ionic liquid, *Journal of Polymer Science Part B-Polymer Physics*. 50 (2012) 1145-1150.
- [8] SA Jenekhe, SJ Tibbetts. Ion-Implantation Doping and Electrical-Properties of High-Temperature Ladder Polymers, *Journal of Polymer Science Part B-Polymer Physics*. 26 (1988) 201-209.
- [9] K Wilbourn, RW Murray. Electrochemical Doping Reactions of the Conducting Ladder Polymer Benzimidazobenzophenanthroline (Bbl), *Macromolecules*. 21 (1988) 89-96.
- [10] JE Anthony, A Facchetti, M Heeney, SR Marder, X Zhan. n-Type Organic Semiconductors in Organic Electronics, *Adv Mater*. 22 (2010) 3876-3892.
- [11] A Babel, SA Jenekhe. Electron transport in thin-film transistors from an n-type conjugated polymer, *Adv Mater*. 14 (2002) 371-374.
- [12] A Babel, SA Jenekhe. N-Channel Field-Effect Transistors from Blends of Conjugated Polymers, *J Phys Chem B*. 106 (2002) 6129-6132.
- [13] A Babel, S Jenekhe. High electron mobility in ladder polymer field-effect transistors, *J.Am.Chem.Soc*. 125 (2003) 13656-13657.
- [14] FS Kim, D Hwang, B Kippelen, SA Jenekhe. Enhanced carrier mobility and electrical stability of n-channel polymer thin film transistors by use of low-k dielectric buffer layer, *Appl.Phys.Lett*. 99 (2011) 173303.
- [15] A Babel, JD Wind, SA Jenekhe. Ambipolar charge transport in air-stable polymer blend thin-film transistors, *Advanced Functional Materials*. 14 (2004) 891-898.
- [16] AL Briseno, FS Kim, A Babel, Y Xia, SA Jenekhe. n-Channel polymer thin film transistors with long-term air-stability and durability and their use in complementary inverters, *Journal of Materials Chemistry*. 21 (2011) 16461-16466.
- [17] AG Manoj, AA Alagiriswamy, KS Narayan. Photogenerated charge carrier transport in p-polymer n-polymer bilayer structures, *J.Appl.Phys*. 94 (2003) 4088-4095.
- [18] MM Alam, SA Jenekhe. Efficient solar cells from layered nanostructures of donor and acceptor conjugated polymers, *Chemistry of Materials*. 16 (2004) 4647-4656.
- [19] V Gowrishankar, CK Luscombe, MD McGehee, JM Frechet. High-efficiency, Cd-free copper-indium-gallium-diselenide/polymer hybrid solar cells, *Solar Energy Mater.Solar Cells*. 91 (2007) 807-812.
- [20] T Matsui, H Mori, Y Inose, S Kuromiya, K Takano, M Nakajima, et al. Efficient optical terahertz-transmission modulation in solution-processable organic semiconductor thin films on silicon substrate, *Japanese Journal of Applied Physics*. 55 (2016) 03DC12.

- [21] F Jahantigh, SMB Ghorashi, AR Belverdi. A first principle study of benzimidazobenzophenanthrolin and tetraphenyldibenzoperiflanthene to design and construct novel organic solar cells, *Physica B-Condensed Matter*. 542 (2018) 32-36.
- [22] H Sun, M Vagin, S Wang, X Crispin, R Forchheimer, M Berggren, et al. Complementary Logic Circuits Based on High-Performance n-Type Organic Electrochemical Transistors, *Adv Mater*. 30 (2018) 1704916.
- [23] P Bornozy, MS Prevot, X Yu, N Guijarro, K Sivula. Direct Light-Driven Water Oxidation by a Ladder-Type Conjugated Polymer Photoanode, *J.Am.Chem.Soc.* 137 (2015) 15338-15341.
- [24] C Bishop, *Vacuum Deposition onto Webs, Films and Foils*, 2nd Edition, 2011.
- [25] S Janietz, D Sainova. Significant improvement of the processability of ladder-type polymers by using aqueous colloidal dispersions, *Macromolecular Rapid Communications*. 27 (2006) 943-947.
- [26] AL Briseno, SCB Mannsfeld, PJ Shamberger, FS Ohuchi, Z Bao, SA Jenekhe, et al. Self-assembly, molecular packing, and electron transport in n-type polymer semiconductor nanobelts, *Chemistry of Materials*. 20 (2008) 4712-4719.
- [27] S Hirvonen, M Manttari, V Wigren, M Salomaki, C Kvarnstrom, H Tenhu. A novel method to prepare water dispersible poly(benzimidazobenzophenanthroline) (BBL) by partial substitution of chain ends with poly(ethylene oxide), *Colloid Polym.Sci.* 289 (2011) 1065-1072.
- [28] S Hirvonen, T Rossi, M Karesoja, E Karjalainen, H Tenhu. Thermally responsive particles of poly(benzimidazobenzophenanthroline) modified with poly(N-isopropylacrylamide), *Colloid Polym.Sci.* 293 (2015) 2957-2965.
- [29] R Latonen, A Osterholm, C Kvarnstrom, A Ivaska. Electrochemical and Spectroelectrochemical Study of Polyazulene/BBL-PEO Donor-Acceptor Composite Layers, *Journal of Physical Chemistry C*. 116 (2012) 23793-23802.
- [30] M Salomaki, T Peltonen, J Kankare. Multilayer films by spraying on spinning surface - Best of both worlds, *Thin Solid Films*. 520 (2012) 5550-5556.
- [31] G Jellison, F Modine. Parameterization of the optical functions of amorphous materials in the interband region, *Appl.Phys.Lett.* 69 (1996) 371-373.
- [32] S Hirvonen, M Karesoja, E Karjalainen, S Hietala, P Laurinmaki, E Vesanen, et al. Colloidal properties and gelation of aqueous dispersions of conductive poly(benzimidazobenzophenanthroline) derivatives, *Polymer*. 54 (2013) 694-701.
- [33] S Kraner, C Koerner, K Leo, E Bittrich, K- Eichhorn, Y Karpov, et al. Dielectric function of a poly(benzimidazobenzophenanthroline) ladder polymer, *Physical Review B*. 91 (2015) 195202.

[34] MM Alam, SA Jenekhe. Conducting ladder polymers: Insulator-to-metal transition and evolution of electronic structure upon protonation by poly(styrenesulfonic acid), *J Phys Chem B*. 106 (2002) 11172-11177.

[35] T Zheng, F Badrun, I Brown, D Leopold, T Sandreczki. Correlation of electron spin concentration and conductivity in the ladder polymer BBL as a function of electrochemical potential, *Synth.Met.* 107 (1999) 39-45.

[36] T Yohannes, H Neugebauer, SA Jenekhe, NS Sariciftci. Multiple reduction states with different conductivities of polybenzimidazobenzophenanthroline (BBL) studied with infrared spectroelectrochemistry, *Synth.Met.* 116 (2001) 241-245.

[37] J BREDAS, R SILBEY, D BOUDREAUX, R CHANCE. Chain-Length Dependence of Electronic and Electrochemical Properties of Conjugated Systems - Polyacetylene, Polyphenylene, Polythiophene, and Polypyrrole, *J.Am.Chem.Soc.* 105 (1983) 6555-6559.

[38] S Jenekhe, S Yi. Efficient photovoltaic cells from semiconducting polymer heterojunctions, *Appl.Phys.Lett.* 77 (2000) 2635-2637.